Myosin Ib modulates the morphology and the protein transport within multi-vesicular sorting endosomes

Laura Salas-Cortes[1,*], Fei Ye[2,*], Danièle Tenza[1], Claire Wilhelm[3], Alexander Theos[4], Daniel Louvard[1], Graça Raposo[1] and Evelyne Coudrier[1,‡]

[1]Institut Curie, CNRS UMR144, 26 rue d'Ulm, 75248, Paris, Cedex 05, France
[2]E363 INSERM, Faculté de Médecine, Necker, 156 Rue de Vaugirard, 75015, Paris, France
[3]Laboratoire des milieux désordonnés et hétérogènes, Universite Pierre et Marie Curie, Boite 86, 4 Place Jussieu, 75252 Paris Cedex 05, France
[4]Department of Pathology and Laboratory Medicine, University of Pennsylvania, 3451 Walnut Street, Philadelphia, PA 19104, USA
*These authors contributed equally to this work
‡Author for correspondence (e-mail: coudrier@curie.fr)

Accepted 2 August 2005
Journal of Cell Science 118, 4823-4832 Published by The Company of Biologists 2005
doi:10.1242/jcs.02607

Summary

Members of at least four classes of myosin (I, II, V and VI) have been implicated in the dynamics of a large variety of organelles. Despite their common motor domain structure, some of these myosins, however, are non processive and cannot move organelles along the actin tracks. Here, we demonstrate in the human pigmented MNT-1 cell line that, (1) the overexpression of one of these myosins, myosin 1b, or the addition of cytochalasin D affects the morphology of the sorting multivesicular endosomes; (2) the overexpression of myosin 1b delays the processing of Pmel17 (the product of murine silver locus also named GP100), which occurs in these multivesicular endosomes; (3) myosin 1b associated with endosomes co-immunoprecipitates with Pmel17. All together, these observations suggest that myosin 1b controls the traffic of protein cargo in multivesicular endosomes most probably through its ability to modulate with actin the morphology of these sorting endosomes.

Keys words: Actin cytoskeleton, Biogenesis of melanosomes, Membrane traffic, Endocytosis

Introduction

Internalised molecules are sorted from resident proteins and lipids along the endocytic pathway, through a complex series of regulated processes. Besides the well-characterized signal motifs, micro-domains on membranes play an important role for efficient sorting of proteins and lipids (Hopkins et al., 1994; Raiborg et al., 2003; Stoorvogel et al., 1987). The transferrin receptor accumulates in tubules before being recycled to the plasma membrane, while the EGF receptor is sequestered in membrane invaginations that give rise to internal vesicles of multi-vesicular endosomes (MVEs, also named multi-vesicular bodies) before its degradation in lysosomes (Hopkins et al., 1994; Raiborg et al., 2003). Compelling evidence from several laboratories indicate that microtubules and associated molecular motors of the dynein and kinesin families are involved in the tubulation of organelles and thereby might contribute to sorting events (Koster et al., 2003; Roux et al., 2002). The participation of actin networks and myosins in different steps of the secretory and endocytic pathways were also investigated but the role of these networks and their associated motors as mechanical devices for sorting processes has only been studied recently.

The acto-myosin generated forces could help to cluster the cargos prior to their transport. For example, the class VI myosin, which binds adaptors proteins containing PDZ domains, such as Dab2 or GIPC, has been proposed to cluster receptors with PDZ-binding motifs in clathrin-coated regions (Hasson, 2003). Acto-myosin tension might also drive morphological changes that could contribute to the formation of micro-domains involved in the sorting process. In this context, in *Dictyostelium discoidum* the knockout of two genes encoding class I myosins, myoA and myoB, leads to a disordered morphology of sorting recycling endosomes (Neuhaus and Soldati, 2000).

We have previously reported that another myosin from class I, myosin Ib (Myo1b, also named myosin I alpha or Myr1), participates in the cytoplasmic distribution of endosomes and lysosomes and in the delivery of internalised molecules to lysosomes in mammalian cells (Cordonnier et al., 2001; Raposo et al., 1999). Despite the involvement of this myosin in the traffic along the endocytic pathway, Myo1b is unable to move endocytic compartments on actin filaments in vivo (Cordonnier et al., 2001). However, Myo1b, together with actin, might drive morphological changes of the endocytic compartments, similarly to myoA and myoB in *Dictyostelium discoidum.* It might also act with actin as a dynamic scaffold and be involved in the sorting of specific cargos.

To investigate further the mechanism by which Myo1b contributes to the traffic of internalized molecules towards the lysosomes, we used the pigmented human melanoma cell line MNT-1, which displays a well defined endocytic system. In these cells, endosomes that were traced with gold-labelled bovine serum albumin 15 minutes post uptake and displayed bilayered clathrin coats and internal vesicles, are intermediates for proteins transported to lysosomes and for proteins involved in the biogenesis of melanosomes (Raposo

and Marks, 2002; Raposo et al., 2001). These endosomes, which had a defined structure and were involved in targeting of proteins to two different organelles, present the hallmark of sorting endosomes (Raiborg et al., 2003; Raposo and Marks, 2002; Raposo et al., 2001; Sachse et al., 2002). We will refer to these compartments as early sorting MVEs in the present study. We report here that overexpression of Myo1b or the inhibition of actin dynamic by drugs affect the morphology of these early sorting MVEs.

One peculiarity of the MNT-1 cellular model is the expression of Pmel17, a melanosome-specific protein (and the product of murine silver locus, also named GP100) that transits in these early sorting MVEs. After its biosynthesis Pmel17 is delivered to early sorting MVEs where, concomitantly or after its delivery, it is cleaved by a furin-like proprotein convertase (Berson et al., 2001; Berson et al., 2003). This cleavage leads to the formation of intra-lumenal fibrils that characterizes stage-II premelanosomes. Using this unique feature of the MNT-1 model, we investigated the contribution of Myo1b in the trafficking and the processing of Pmel17 in the early sorting MVEs. We report here that, the overexpression of Myo1b delays the processing of Pmel17 and thereby impairs the formation of the intra-lumenal fibrils in stage-II premelanosomes, and that Myo1b associated with endosomes co-immunoprecipitates with Pmel17. All together, these observations indicate that Myo1b and actin are involved in the morphological organisation of the early sorting MVE and in the transfer of cargo proteins such as Pmel17 towards internal vesicles of these endosomes.

Materials and Methods

Antibodies

Monoclonal antibodies HMB50 and HMB45 directed against the N-terminus of Pmel17 were obtained from Neomarkers (Fremont, CA). Monoclonal antibody directed against early endosome antigen 1 (EEA1) was obtained from BD Biosciences (San Diego, CA), monoclonal antibody directed against green fluorescent protein (GFP) from Molecular Probes (Eugene, OR) and monoclonal anti-tubulin from Amersham (Bioscience Europe GmbH). Polyclonal anti-Rab5 antibodies were a generous gift from M. Zerial (Max-Plank-Institute, Dresden, Germany), anti-Rab7 antibodies a generous gift from P. Chavrier (Institut Curie, Paris, France), αpep13h antibodies (Berson et al., 2001) a generous gift from M. Marks (University of Pennsylvania, Philadelphia, PA), anti-β-actin antibodies a generous gift from C. Chaponnier (Geneva University, Geneva, Switzerland). Two rabbit polyclonal antibodies directed against Myo1b were generated against peptides with the sequence (CSFRTVEAKQEKVSTTLNVAQAT) (SE7995) as previously described by Tang and Ostap (Tang and Ostap, 2001) and the C-terminal sequence (CKRKNNRLLEVAVP) (SE5237).

Cell culture and isolation of stable transformants

Cells of the human melanoma MNT-1 cell line were grown in MNT-1 culture medium, consisting of Dulbecco's modifies Eagle's medium (DMEM, Gibco-BRL Life Technology, Paisley, UK) supplemented with 10% AIMV medium (Gibco-BRL Life Technology), 20% foetal calf serum (Gibco-BRL Life Technology), penicillin (10 units/ml) and streptomycin (10 mg/ml) (Gibco-BRL Life Technology). Transfection with the recombinant DNA constructs encoding EGFP, EGFP-Myo1b and EGFP-Myo1b-Tail (Raposo et al., 1999), and isolation of stable transformants were performed as described by Durrbach et al. (Durrbach et al., 2000). Three cellular clones producing EGFP (EGFP cells), three cellular clones producing EGFP-Myo1b (EGFP-Myo1b cells), and four cellular clones producing EGFP-Myo1b-Tail (EGFP-Myo1b-Tail cells) were selected and permanently grown in the MNT-1 culture medium in which penicillin-streptomycin was replaced by 0.7 mg/ml Geneticin (Gibco-BRL Life Technology). These cellular clones were treated overnight with 10 mM sodium butyrate (Sigma-Aldrich, France) before experiments.

HeLa cells were maintained in DMEM supplemented with antibiotics. Stable transfectants were generated with pCI-Pmel17 (Berson et al., 2001; Berson et al., 2003) after transfection using FuGene6 (Roche Biochemicals, Indianapolis, IN) as previously described (Marks et al., 1995).

Cell homogenate and membrane fractionation

Membrane fractionation

Wild-type-expressing, EGFP-expressing and EGFP-Myo1b-expressing cells were grown 4 days in a 150 cm^2 flask, washed with 5 ml of homogenisation buffer (HB) containing 50 mM imidazole pH 7.4, 0.25 M sucrose, 1 mM EDTA, 0.5 mM EGTA, 5 mM $MgSO_4$, 1 mM DTT, 150 μg/ml casein from bovine milk and protease inhibitors (Sigma Aldrich, France). They were then scraped off into 5 ml HB and homogenized by passing them twice through a cell cracker. Post-nuclear supernatant (PNS) collected after a 7-minute centrifugation at 600 ***g*** was then centrifuged for 5 minutes at 2500 ***g*** to separate the membrane-rich fraction and the cytosol (S1) from melanosomes. A membrane-rich fraction (P2) was collected after centrifugation of the supernatant (S1) for 20 minutes at 100,000 ***g***.

Magnetic endosomes

To isolate magnetic endosomes, MNT-1 cells that had been grown 4 days in a 300 cm^2 flask, were incubated with 1 mM of Fe nanoparticles ($CoFe_2O_4$) coated with negatively charged citrate ligand for 1 hour at 4°C. They were then chased for 30 minutes at 37°C as described by Wilhelm et al. (Wilhelm et al., 2002). Cells were homogenized as described above, and PNS was loaded onto a magnetic column (5 ml/high magnetic field gradient). The non-magnetic fraction (NMF) was eluted first. The magnetic fraction (MF) was collected in the absence of magnet, and washed and magnetized twice more in 5 ml HB before its final collection in 200 μl HB.

Metabolic labelling, immunoprecipitation, and immunoblotting

Metabolic labelling

Cells were harvested, starved of methionine and cysteine, pulse-labelled for 10 minutes with [^{35}S]methionine-cysteine labelling mix (200 μCi), chased with excess methionine and cysteine for indicated periods of time and washed with PBS. After chase incubation, culture medium was collected and clarified by centrifugation.

Immunoprecipitation

Cells that had been grown for 4 days and [^{35}S]methionine-cysteine metabolically labelled or not, were scraped off and lysed on ice in 50 mM Tris pH 7.5, containing 300 mM NaCl, 1 mM EDTA (lysis buffer) and 1% Triton X-100. The cell lysate was cleared by centrifugation for 20 min at 20,000 ***g***, and by absorption with 25 μl of protein G sepharose beads (Amersham Bioscience Europe GmbH). The immuno-complex formed overnight (by incubating the pre-cleared cell lysate with 5 μg of purified antibody at 4°C) was absorbed by 25 μl protein G sepharose, washed 3× with lysis buffer containing 1% Triton X-100, 3×with lysis buffer containing 0.1% Triton X-100, analysed by SDS-PAGE and immunoblotting.

Immunoblotting

Proteins separated by SDS-PAGE were transferred to nitrocellulose

membranes in the presence of 20 mM Tris, 150 mM glycine and 0.05% SDS. Detection of antibodies was performed using the chemiluminescence blotting substrate from Roche Applied Sciences (Meylan, France) or Super Signal West Pico Chemiluminescent substrate from Pierce Biotechnology (Rockford, IL, USA).

Immunofluorescence microscopy

Cells were grown 4 days on cover-slips, fixed in PBS containing 3% paraformaldehyde and 0.025% glutaraldehyde, and permeabilized for 10 minutes in PBS containing 0.05% saponin. Cells were then incubated 30 minutes with primary antibodies, followed by a 30-minute incubation with FITC-conjugated or Cy3-conjugated antibodies (Rockland immunochemicals for research, Gilbertsville, PA 19525). Phalloidin (0.5 μg/ml) conjugated with TRITC (Sigma-Aldrich) was used to label F-actin. The cells were viewed with a confocal laser-scanning microscope (Leica, Vienna, Austria).

Electron microscopy

For conventional electronic microscopy, EGFP-Myo1b cells grown 4 days on cover slips were fixed with 2.5% glutaraldehyde in 0.066M cacodylate buffer for 3 hours at room temperature. After several washes with cacodylate buffer, cells were post-fixed with 2% OsO4 for 45 minutes, dehydrated with increasing concentrations of ethanol and embedded in Epon^{TM}. Ultra-thin sections were counterstained with 4% uranyl acetate in methanol for 5 minutes.

Ultra-cryomicrotomy and immunogold labelling was performed as previously described (Raposo et al., 1997). Cells were fixed with a mixture of 2% PFA and 0.125% glutaraldehyde for 3 hours at room temperature. Cells were pelleted, washed with 50 mM PBS-glycine and embedded in 10% gelatine at 37°C. After solidification on ice, small 1-mm^3 blocks were prepared, infused in 2.3 M sucrose and frozen in liquid nitrogen. Ultra-thin cryosections were retrieved with a mixture of 2% methyl-cellulose–2.3 M sucrose (vol/vol), thawed and single or double immunogold labelling was performed. Antibodies were detected directly with protein-A gold-conjugates (purchased from Department of Cell Biology, Institute for Biomembranes, Utrecht, Netherlands). Sections were cut with UCT and FCS Leica microtomes, and viewed and photographed with a TEM Philips CM 120 (FEI company, Eindoven, The Netherlands). Negatives were scanned with a Rotatif scanner (Highscan-Eurocore).

Results

Expression of EGFP-Myo1b perturbs the cellular distribution of endosomes

Endogenous MYO1B was found to be concentrated in dynamic membrane areas of MNT-1 cells that were enriched with actin cytoskeleton as previously reported for other cell types (Raposo et al., 1999; Tang and Ostap, 2001) (Fig. 1A-C arrows). In addition, MYO1B was associated with punctate structures in the cytoplasm. Some of these structures co-distributed with EEA1 (early endosome antigen 1), one of the Rab5 effectors that is abundant in early endosomes (Fig. 1D-F, see arrows). Thus, consistent with our previous observation in the hepatoma cell line, a pool of MYO1B is associated to the endosomes of MNT-1 cells (Raposo et al., 1999).

To investigate the role of MYO1B in protein-trafficking along the endocytic pathway, we isolated a cellular clone derived from MNT-1 cells that expressed the EGFP-tagged rat Myo1b isoform c. The EGFP-Myo1b hybrid protein showed similar biochemical properties than the endogenous human MYO1B. Both were associated with cellular fractions enriched in membrane vesicles. Polyclonal anti-Myo1b antibodies

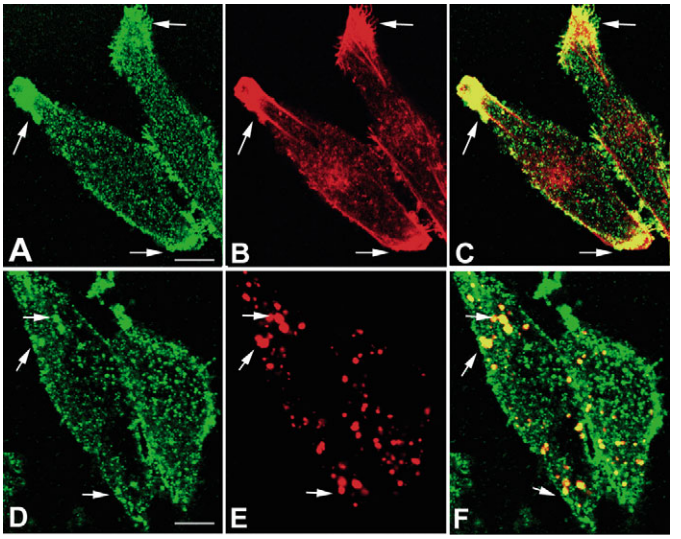

Fig. 1. MYO1B co-distributes with actin filaments at the cell periphery and partially with endosomes in MNT1 cells. (A-C) MNT-1 cells were co-labelled with affinity-purified polyclonal anti-Myo1b antibodies (SE5237) and phalloidin and analysed using confocal microscopy. Same optical section throughout the focal plane of the nucleus of one MNT-1 cell is shown for (A) Myo1b and (B) actin. Overlay of A and B is shown in C. Arrows show membrane areas enriched in actin filaments. Bar, 2.2 μm. (D-F) MNT-1 cells were co-labelled with affinity-purified polyclonal anti-Myo1b antibody (SE5237) and anti-EEA1 antibody. Same optical section throughout the focal plane of the nucleus of one MNT-1 cell for (D) Myo1b and (E) EEA1. An overlay of D and E and is shown in F. Arrows imdicate the partial co-distribution between endosomes and Myo1b. Bar, 1.9 μm.

raised against a specific peptide of the motor domain (Tang and Ostap, 2001) immunodetected a broad protein pattern with a size of 120 to 130 kDa in the membrane-vesicle-enriched fraction P2, isolated from EGFP-Myo1b cells (Fig. 2A). This protein-mobility pattern very probably corresponds to one or several MYO1B isoforms (Ruppert et al., 1993). Anti-Myo1b antibodies revealed also a protein of the size compatible with the size of the EGFP-Myo1b hybrid protein. Indeed, this protein was also detected by anti-GFP antibodies (data not shown). In agreement with previous observations (Tang and Ostap, 2001), MYO1B was resistant to extraction with Triton X-100 and required ATP in addition to detergent to partially dissociate from the membrane-vesicle-enriched fraction P2 (Fig. 2A). Similarly, EGFP-Myo1b dissociated from P2 after the addition of ATP to the detergent (Fig. 2A).

EGFP-Myo1b accumulated at the plasma membrane of MNT-1 cells in dynamic membrane areas that were enriched with actin cytoskeleton, such as membrane protrusions (Fig. 2B-D see arrow). EGFP-Myo1b was rarely associated with punctate structures in the cytoplasm and co-distribution with endosomes was difficult to determine at light-microscopic level. However, EGFP-Myo1b was detected at EM-level close to EEA1-labelled endosomes and in the magnetic fraction enriched in endosomes (Figs 3C and 9A). Furthermore, expression of EGFP-Myo1b in MNT-1 cells appeared to modify the distribution of the endocytic compartments labelled with anti-EEA1 antibodies. Endosomes accumulated in the

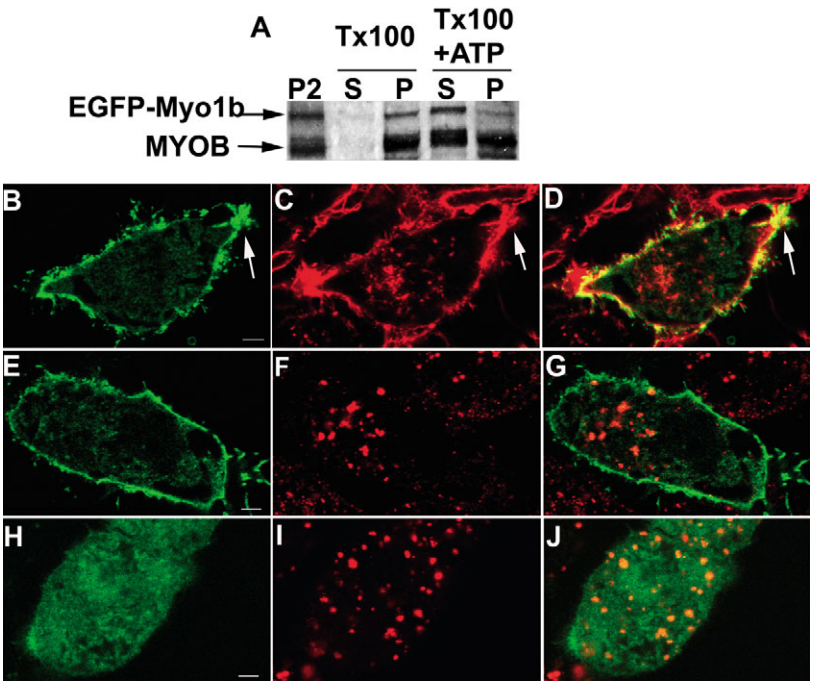

Fig. 2. Expression of EGFP-Myo1b induces the re-distribution of endosomes in the perinuclear region of MNT-1 cells. (A) 20 μg of the membrane-enriched fraction P2, as well as pellets and supernatants that had been collected after high-speed centrifugation of 20 μg P2 treated with 1%Triton X-100 or 1%Triton X-100 with 5 mM ATP for 30 minutes at 4°C, were separated by 7% SDS-PAGE and transferred on nitrocellulose membranes. The membrane was probed with anti-Myo1b antibody (SE7995). Endogenous MYO1B and EGFP-Myo1b are both released after treatment with Triton X-100 supplemented with ATP. (B-J) EGFP-Myo1b-expressing and EGFP-expressing cells (B-G and H-J, respectively) were labelled with (B-D) phalloidin, (E-J) anti-EEA1 antibody and analysed by confocal microscopy. Same confocal section throughout the focal plane of the nucleus for the expression of (B) EGFP-Myo1b and (C) actin, (E) EGFP-Myo1b and (F) EEA1, (H) EGFP and (I) EEA1. (D) Overlay of B and C. (G) Overlay of E and F. (J) Overlay of H and I. The arrows show a membrane area enriched in actin filaments. Notice that overexpression of EGFP-Myo1b affects the cellular distribution of the endocytic compartments. Bars, 2.2 μm (B,E) and 1.9 μm (H).

perinuclear region in 73% of the cells expressing EGFP-Myo1b and only in 11% of the EGFP cells (Fig. 2, compare F and G with I and J, respectively).

Expression of EGFP-Myo1b modifies the morphology of early sorting MVEs

We next analysed how expression of EGFP-Myo1b affected the endosomes of MNT-1 cells at the ultra-structural level. MNT-1 cells exhibit the different compartments of the endocytic pathway that consist of small tubulovesicular endosomes accessible for internalised molecules within 5 to 10 minutes, early sorting MVEs accessible for internalised molecules within 20 minutes, MVEs and also melanosomes at different stages of maturation (Raposo et al., 2001). As determined by conventional electron microscopy, the expression of EGFP-Myo1b in MNT-1 cells, resulted often in the accumulation in the perinuclear region of early sorting MVEs, with a characteristic electron-dense coat at their cytosolic side (Fig. 3A). Consistent with previous reports, immunogold-labelling on ultra-thin cryosections of EGFP-Myo1b cells revealed the presence of EEA1 in the non-coated regions of these early sorting MVEs (Fig. 3B, see arrows). Interestingly, small membrane extensions and vesicles in their vicinity appeared to be more abundant on endosomes from EGFP-Myo1b-expressing cells compared with those of wild-type cells (Fig. 3B versus 3E). EEA1-positive compartments that are re-distributed upon EGFP-Myo1b overexpression (Fig. 2F) might correspond to clusters of early sorting MVEs, which display increased amounts of small protrusions (Fig. 3A,B).

We also analysed the distribution of EGFP-Myo1b at the EM level. Low amounts were detected under the above described experimental conditions. However, EGFP-Myo1b appeared restricted to small vesicle-like structures in the vicinity of the early sorting MVEs on ultra-thin cryosections (Fig. 3C). Some of these structures may correspond to cross sections of the small protrusions. To better evaluate the distribution of EGFP-Myo1b, we used whole-mount immunogold labelling on cells in which endosomes had been crosslinked with internalised HRP (Stoorvogel et al., 1996). This method has been used previously to detect Myo1b on endosomes of BWTG3 cells (Raposo et al., 1999). EGFP-Myo1b was detected on the vacuolar domain but appeared enriched on the small tubular membrane extension of the early sorting MVEs (Fig. 3D).

If Myo1b is driving morphological changes of these endocytic compartments then it might do this together with actin. Interestingly, EEA1-labelled endosomes that were observed at the light microscopic level co-distributed partially with actin filaments (Fig. 4A-C see arrows) and a consistent pool of actin was found in the close vicinity of these endosomes when they were observed at the electron microscopic level (Fig. 3E see long arrows). Particularly, actin was detected at the opposite side of the clathrin coated areas, where the small membrane vesicles and small tubular extensions were observed (Fig. 3E see small arrows). Furthermore, the treatment of MNT-1 cells with cytochalasin D induced the re-distribution of EEA1-labelled endosomes in the perinuclear region in close vicinity of actin patches (Fig. 4D,E,F see arrows) and facilitated the visualisation of the tubular extensions at the electron microscopic level (Fig. 3F see arrows).

These observations indicate that a small fraction of EGFP-Myo1b is associated with EEA1-labelled endosomes. Some of these endosomes are early sorting MVEs, as judged by electron microscopy. Furthermore, overexpression of EGFP-Myo1b, or cytochalasin D treatment impairs the cellular distribution and the morphology these compartments.

Expression of EGFP-Myo1b perturbs the cellular distribution and the maturation of Pmel17

The delocalization and the morphological changes of the early sorting MVEs induced by the expression of EGFP-Myo1b may

consequently perturb the transport of proteins that are passing through these endocytic compartments. Therefore, we analysed the cellular distribution and the maturation of Pmel17, which is processed in early sorting MVEs in their transition to stage-II melanosomes (Berson et al., 2001; Berson et al., 2003; Raposo et al., 2001). Intracellular compartments labelled with HMB50, an antibody that detects Pmel17, were dispersed from the cell periphery to the perinuclear region in all EGFP cells analysed, while they were mostly concentrated in the perinuclear region in 56% of EGFP-Myo1b cells (Fig. 5A versus 5B). However, consistent with a previous report (Raposo et al., 2001), the distribution of Pmel17 and specific markers of endosomes did not overlap when cells were examined through a light microscope. In that report, the majority of Pmel17 in MNT-1 cells was associated with premelanosomes and mature melanosomes (Raposo et al., 2001). Thus, the Pmel17-positive compartments, which were concentrated in the perinuclear region of EGFP-Myo1b cells, might correspond to premelanosomes and melanosomes. By contrast, it has been reported that the majority of Pmel17 is associated with a subset of late endosomes in HeLa cells transiently expressing Pmel17 (Berson et al., 2001). We isolated a cellular clone, derived from HeLa cells and expressing Pmel17. After 20 minutes of internalisation, Pmel17 co-distributed with EGF (data not shown). Interestingly, the transient expression of EGFP-Myo1b in HeLa cells expressing Pmel17 induced the perinuclear re-distribution of Pmel17 (Fig. 5 compare C with D). Overexpression of EGFP-Myo1b alters, therefore, the distribution of Pmel17 associated with endosomes in HeLa cells, and with mature and immature melanosomes in MNT-1 cells. We hypothesised that the disrupted localisation of Pmel17 associated with mature and immature melanosomes in MNT-1 cells is a consequence of the altered trafficking of Pmel17 in endosomes.

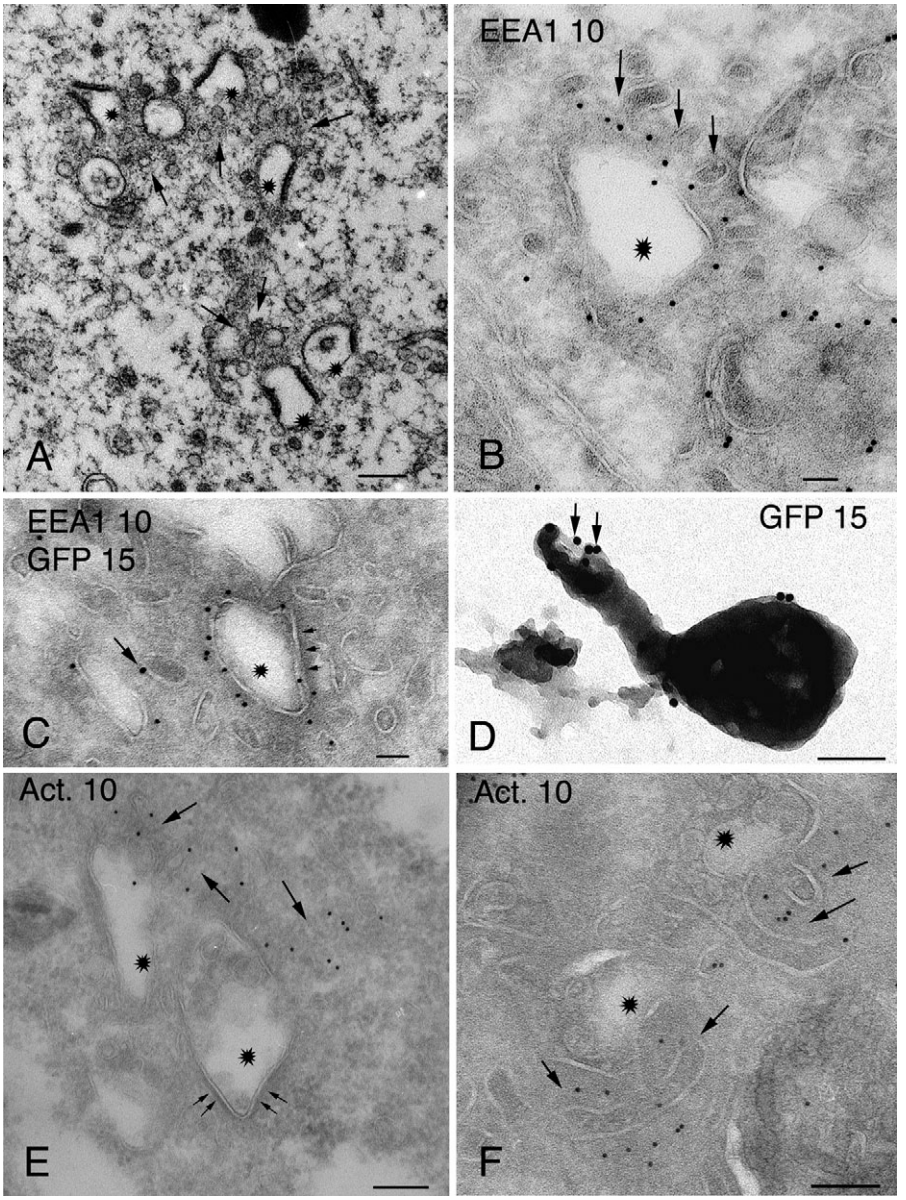

Fig. 3. Expression of EGFP-Myo1b and cytochalasin D affect the distribution and morphology of endosomes. (A) Ultra-thin section of Epon-embedded EGFP-Myo1b cells. Notice the clustered vacuolar endosomes with an electron-dense coat (stars). Ultra-thin cryosections of EGFP-Myo1b cells singly immunogold-labelled for EEA1 (B) or doubly immunogold-labelled for EEA1 and EGFP (C). Notice the numerous vesicular and tubular extensions at the opposite site of the coats in B and C (large arrows). (D) EGFP-Myo1b was visualized on whole-mounted cells. An endosome filled with HRP and immunogold-labelled for GFP is shown. Labelling is observed on the vacuolar domain and mostly concentrated in an extending tubule (arrows). (E) Ultra-thin cryosections of nontransfected cells immunogold-labelled for actin. Actin (long arrows) is detected on small tubulovesicular elements close to the endosomal vacuoles (stars) at the opposite site of the coated areas (short arrows). (F) Ultra-thin cryosection of MNT-1 cells immunogold-labelled for actin and treated with 0.4 μM cytochalasin D for 90 minutes. Actin is detected at the cytosolic side of tubular structures (arrows). Bars, 200 nm.

To test this hypothesis, we followed the processing of Pmel17 in MNT-1 cells. Pmel17 is an integral membrane protein. It is synthesised in the endoplasmic reticulum as precursor P1, O-linked-glycan- and N-linked-glycan-modified in the Golgi complex to result in the precursor P2, and cleaved in a post-Golgi pre-lysosome compartment into two disulfide-linked subunits. These subunits include a C-terminal 28 kDa Mβ subunit that contains part of the lumenal domain, the entire transmembrane and cytoplasmic domains and an 80 kDa Mα subunit with the remaining N-terminal region of the lumenal

domain (Fig. 6A) (Berson et al., 2001). We compared the processed forms of Pmel17 in EGFP cells with that in EGFP-Myo1b cells. P1 and P2 precursors and the two disulfide-linked subunits Mα and Mβ were immunoprecipitated together with a monoclonal antibody directed against the N-terminus of Pmel17, HMB50. The amounts of Mα and Mβ immunoprecipitated from EGFP-Myo1b cells in these experimental conditions appeared to be lower than the amount immunoprecipitated from EGFP-expressing cells (Fig. 6B). Conversely, the amount of the precursor P2 was slightly increased in EGFP-Myo1b cells compared with that of EGFP cells (Fig. 6B). To confirm this first observation, which suggests that Myo1b can control the transport of Pmel17 leading to its processing, we compared the posttranslational processing of Pmel17 in EGFP-Myo1b cells with that in EGFP-expressing cells. In agreement with the previous report by Berson and colleagues (Berson et al., 2001), the endoplasmic reticulum precursor P1 immunoprecipitated 10 minutes after pulse-labelling, whereas P2 immunoprecipitated as a broad protein pattern that overlapped with the P1 precursor after 10 minutes of pulse-labelling and 30 minutes of chase (Fig. 6C). Furthermore, Mα, which predominantly immunoprecipitated in a diffuse protein pattern co-migrating with an alternatively spliced form of Pmel17 and Mβ, was detected after 1 hour of chase (Fig. 6C). Consistent with the observations at the steady state, Mβ levels were significantly lower and Mα was hardly detectable in EGFP-Myo1b cells, while levels of the precursor P2 appeared to slightly increase after 1 and 2 hours of chase in the EGFP-Myo1b-expressing cells (Fig. 6C and D).

We next examined whether the delayed cleavage of Pmel17 perturbed the formation of the intralumenal fibrils of stage-II premelanosomes in EGFP-Myo1b cells as previously reported, when cleavage of Pme17 was inhibited by expressing a variant of α1-antitrypsin inhibitor (Berson et al., 2003). Indeed, abortive fibrils were frequently observed in the immature melanosomes of the EGFP-Myo1b cells (Fig. 7). All together these observations suggest that MYO1B controls the processing of Pmel17, leading to the formation of the intralumenal fibrils of stage-II premelanosomes.

MYO1B associated with endosomes co-immunoprecipitates with Pmel17

MYO1B might regulate the trafficking of proteins that pass through the early sorting MVE by controlling the morphology of these compartments as reported above. It might also act as a dynamic scaffold in interacting directly or indirectly with these proteins. Thus, we next investigated whether MYO1B can interact with Pmel17. Anti-GFP antibodies immunoprecipitated EGFP or EGFP-Myo1b from EGFP and EGFP-Myo1b cell lysates respectively (Fig. 8B). In addition, these antibodies precipitated a polypeptide (120 kDa) recognised by anti-Pmel17 antibodies (pep13h) from EGFP-

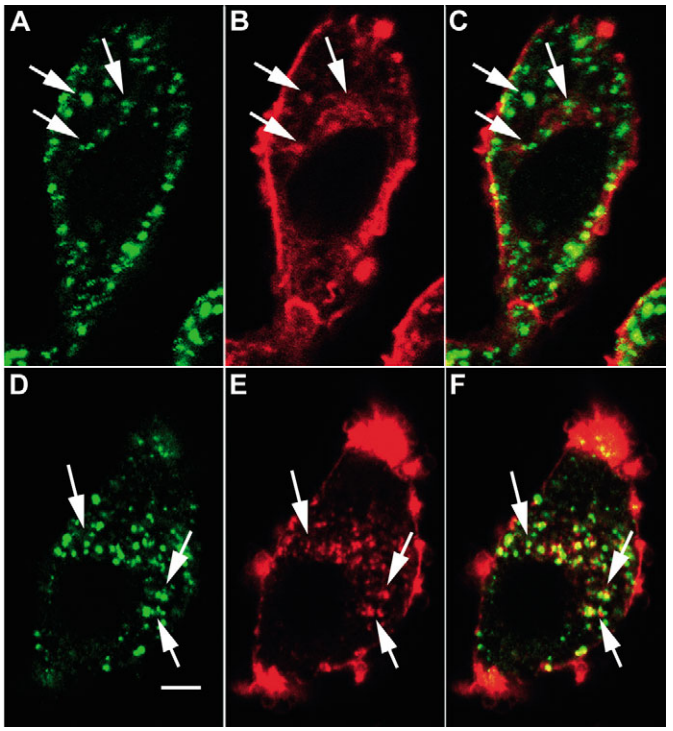

Fig. 4. Cytochalasin D induces the re-distribution of endosomes in the perinuclear region of MNT-1 cells. (A-F) MNT-1 cells that had been treated (D,E,F) or not (A,B,C) with cytochalasin D were co-labelled with anti-EEA1 antibody (A,D), and phalloidin (B,E), and then analysed using confocal microscopy. (A,B) and (D,E) show the same confocal sections throughout the nucleus. (C,F) Overlay of (C) A,B and (F) D,E. Arrows show co-distribution of EEA1-labelled compartments with actin filaments. Bar, 2.8 μm.

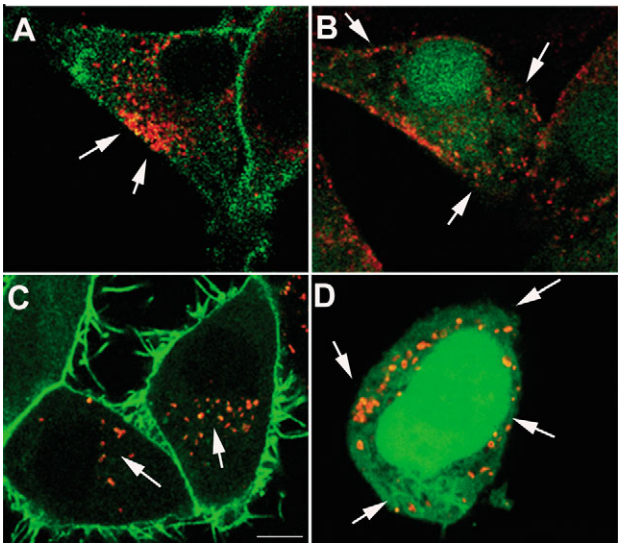

Fig. 5. Expression of EGFP-Myo1b perturbs the cellular distribution of Pmel17. (A,B) EGFP-Myo1b-expressing (A) or EGFP-expressing (B) MNT-1 cells labelled with anti-Pmel17 antibody (HMB50) and analysed by confocal microscopy. Overlay of the optical section through the nucleus shows the distribution of Pmel17 and EGFP-Myo1b (A). Overlay of the optical sections throughout the nucleus showing the distribution of Pmel17 and EGFP (B). (C,D) Pmel17-expressing HeLa cells that had been transiently transfected with cDNA encoding (C) EGFP-Myo1b and (D) EGFP, were labelled with anti-Pmel17 antibody (HMB50) and analysed by confocal microscopy. Overlay of the optical sections through the nucleus show the distribution of (C) Pmel17 and EGFP-Myo1b, and (D) Pmel17 and EGFP. Notice the re-distribution of Pmel17 (arrows) towards the nucleus in EGFP-Myo1b-expressing cells. Bars, 1.9 μm.

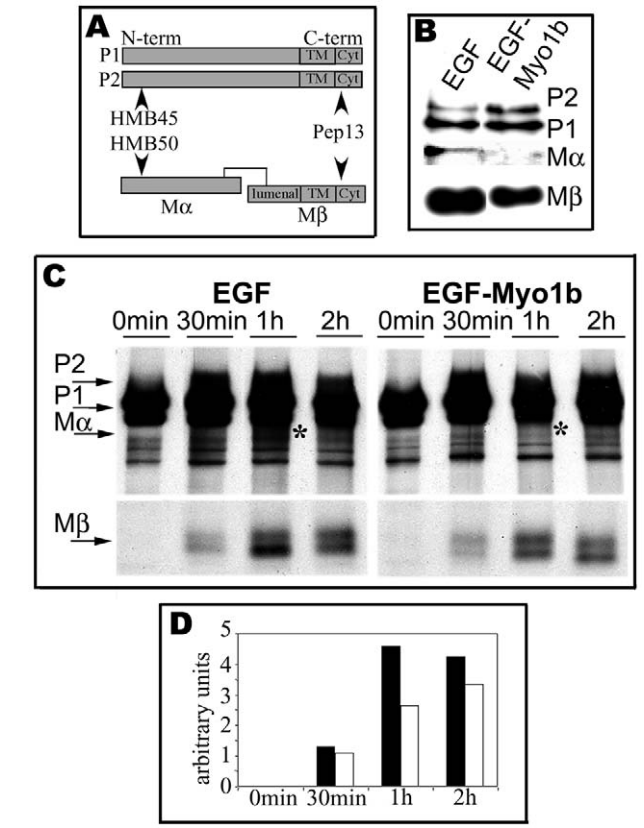

Fig. 6. Expression of EGFP-Myo1b delays the processing of Pme17. (A) Schematic representation of Pmel17 and the processed forms proposed by Berson et al. (Berson et al., 2001). Pmel17 is synthesized as type-I integral membrane protein precursor P1 in the endoplasmic reticulum, glycosylated to precursor P2 in the Golgi, and cleaved into two disulfide-linked subunits: a large lumenal subunit Mα and an integral membrane subunit Mβ. Antibodies HMB45 and HMB50 recognize the N-terminus of P1, P2 and Mα. HMB50 immunoprecipitates both Mα and Mβ, because of their disulfide-link. αPEP13 antibody recognizes the C-terminus of P1, P2 and Mβ. (B) Lysates from five million EGFP-expressing or EGFP-Myo1b-expressing cells were immunoprecipitated with HMB50. Precipitates were then analysed by western blotting with HMB45 to detect Mα, and αPEP13 to detect P1, P2 and Mβ. The same membrane was used for the detection of the different polypeptides. One of four representative experiments is shown. (C) EGFP-expressing cells and EGFP-Myo1b cells were metabolically pulse-labelled with [^{35}S]methionine/cysteine for 10 minutes and then chased for 0 minutes, 30 minutes, 1 hour and 2 hours. 25 μCi of cell lysate were then immunoprecipitated with HMB50. Precipitated proteins were analysed by SDS-PAGE and detected by auto-radiography. (D) The relative intensities of Mβ in EGFP and EGFP-Myo1b cells were quantified and expressed in arbitrary units. (C,D) One of three representative experiments is shown.

Myo1b cell lysates but not from EGFP cell lysates (Fig. 8B). This polypeptide, having an apparent molecular mass of 120 kDa, could be the Golgi-modified O- and N-linked glycan precursor of Pmel17, P2 (see Fig. 6A). By contrast, other endosomal proteins, such as Eps15, that have been proposed to interact with actin or EEA1 and clathrin were not detected in these immunoprecipitates (data not shown). Conversely, when immunoprecipitates were prepared with the monoclonal antibody HMB50 against Pmel17, MYO1B and EGFP-Myo1b were detected in precipitates from EGFP-Myo1b cell lysates but EGFP was not detected in precipitate from EGFP-expressing cell lysates (Fig. 8C). The tail-domain at the C-terminus of Myo1b has been postulated to be involved in the interaction of Myo1b with membrane domains (Fig. 8A) (Raposo et al., 1999; Tang and Ostap, 2001). Consistent with this hypothesis, we detected the EGFP-Myo1b-Tail in anti-Pmel17 immunoprecipitates prepared from lysates of MNT-1 cells that overexpressed EGFP-Myo1b-Tail (Fig. 8C).

If the direct or indirect interaction of MYO1B with Pmel17 is involved in the transport of Pmel17, this interaction should take place on endosomes, where sorting and maturation of Pmel17 occurs. Taking advantage of a new method to isolate magnetic endosomes we determined whether

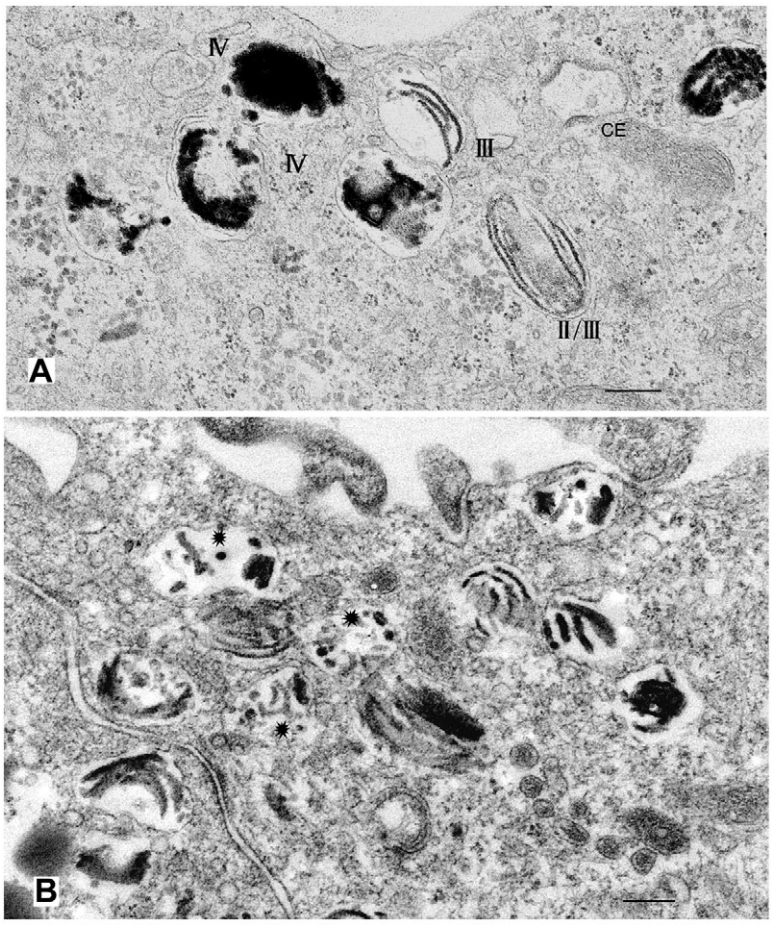

Fig. 7. Morphology of pre-melanosomes is altered upon expression of EGFP-Myo1b. (A) Ultra-thin section of Epon-embedded nontransfected MNT1 cells. Several melanosomal stages (II, III and IV) as well as coated sorting MVEs (CE) are shown. (B) Ultra-thin section of Epon-embedded EGFP-Myo1b cells. Stage-II and stage-III melanosomes show disrupted intraluminal fibrils and abnormal deposits of melanin (stars). Bars, 200 nm.

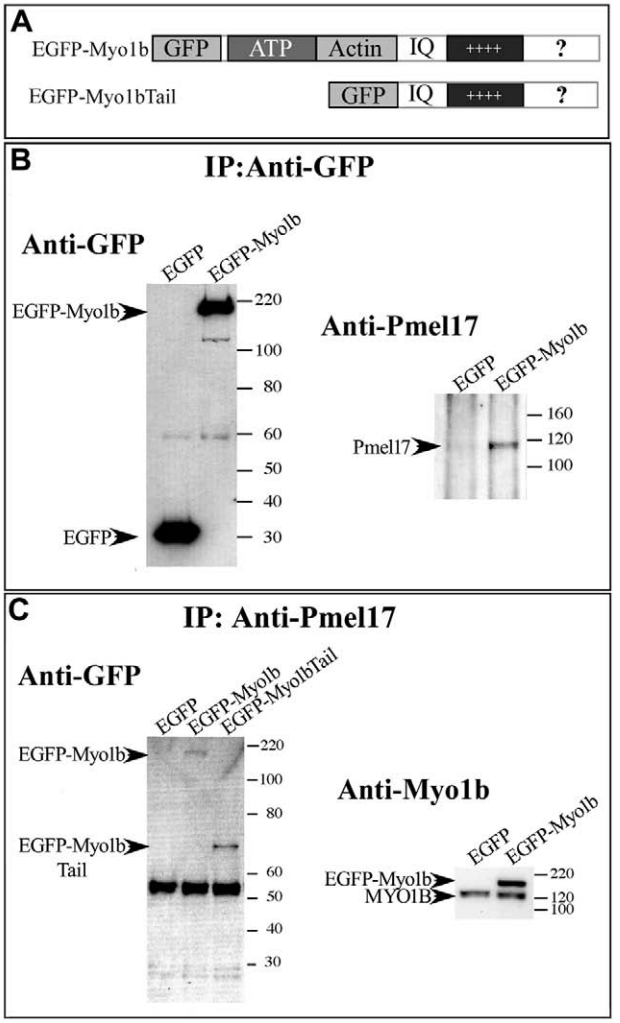

Fig. 8. EGFP-Myo1b and MYO1B co-immunoprecipitate with the precursor P2 of Pmel17. (A) Schematic representation of recombinant EGFP-Myo1b and Myo1b-truncated domains. Myo1b has a motor domain with ATP- and actin-binding sites at the N-terminus and a tail with IQ motifs and a cluster of basic amino acids at the C-terminus. The motor domain was deleted in EGFP-Myo1b-Tail. (B) EGFP or EGFP-Myo1b cell lysates were immunoprecipitated with anti-GFP antibodies and analysed by SDS-PAGE, and western blotting with anti-GFP antibody and the anti-Pmel17 antibody αPep13. (C) EGFP, EGFP-Myo1b and EGFP-Myo1b-Tail cell lysates were immunoprecipitated with the anti-Pmel17 antibody (HMB50) and analysed by SDS-PAGE, and western blotting with anti-GFP antibody. EGFP and EGFP-Myo1b cell lysates immunoprecipitated with HMB50 antibody were also analysed by SDS-PAGE, and western blotting with anti-Myo1b antibody (SE7995). These experiments were repeated three and four times for B and C, respectively.

MYO1B and Pmel17 could co-immunoprecipitate from a fraction enriched in endocytic compartments. Magnetic endosomes were isolated after internalising super paramagnetic nano-particles for 30 minutes (Wilhelm et al., 2002). This magnetic fraction was enriched in specific markers for early endosomes, such as Rab5, and exhibited low amounts of specific markers of late endosomes, such as Rab7, confirming the efficiency of this purification method (Fig. 9A).

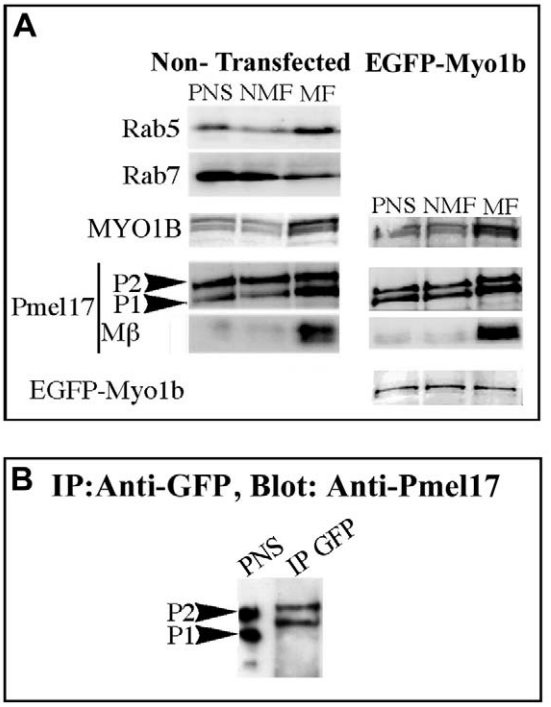

Fig. 9. EGFP-Myo1b and Pmel17 associated to magnetic-endosome co-immunoprecipitate. (A) Post-nuclear supernatant (PNS), non-magnetic (NMF) and magnetic fractions (MF) isolated from wild-type or EGFP-Myo1b cells as described in Materials and Methods, were analysed by SDS-PAGE, and western blotting with anti-Rab5 and anti-Rab7antibodies in the case of wild-type cells, anti-Myo1b (SE7995) and anti-Pmel17 (Pep13h) antibodies for the magnetic fraction of both cell types, and anti-GFP antibodies for the magnetic fraction isolated from EGFP-Myo1b cells. Note that MYO1B as well as P1, P2 and Mβ polypeptides of Pmel17 are present in the magnetic fraction enriched for Rab5, and that EGFP- Myo1b is detected on the magnetic fraction isolated from EGFP-Myo1b cells. (B) Lysate of the magnetic fraction isolated from EGFP-Myo1b cells was immunoprecipitated with anti-GFP antibody and analysed by SDS-PAGE, and western blotting with anti-Pmel17 (Pep13h) antibody. The molecular mass of the immunoprecipitated proteins was compared to the molecular mass of the Pmel17 precursor forms P1 and P2, which had been detected with the same antibody in the post nuclear supernatant (PNS). A polypeptide of the size comparable with P2 co-immunoprecipitates with EGFP-Myo1b.

Endogenous MYO1B was enriched in the magnetic fractions isolated from wild-type and EGFP-Myo1b cells and EGFP-Myo1b was associated to some extend with the fraction isolated from EGFP-Myo1b cells (Fig. 9A). Precursor and mature forms of Pmel17 were also detected in the two magnetic fractions isolated from wild-type or EGFP-Myo1b cells (Fig. 9A). From the magnetic endosomes isolated from EGFP-Myo1b cells, anti-GFP antibody immunoprecipitated two proteins: one with the apparent molecular mass similar to the Pmel17 precursor P2 detected in the post nuclear supernatant (Fig. 9B compare lanes PNS and IP GFP) and one with higher molecular mass than the P2 precursor. This second protein is probably a degradation product because its mobility on the gel was slower than that of the P1 precursor when using the same antibodies for detection in post nuclear supernatant fraction (see lane PNS versus lane IP GFP Fig. 9B). Together, these

observations indicate that, MYO1B and the Pmel17 precursor P2 are associated with the endocytic compartments (which are enriched in Rab5 protein), and bind directly or indirectly to each other. This interaction might occur through the C-terminal tail-domain of MYO1B.

Discussion

Members of several classes of myosins have been implicated in endocytosis in mammals. Myosin VI is required for the traffic of endosomes and clathrin coated vesicles at the cell periphery (Buss et al., 2001; Hasson, 2003). Myosin V is involved in transferrin recycling and Myo1b contributes to the delivery of internalised molecules to lysosomes (Hales et al., 2002; Raposo et al., 1999; Rodriguez and Cheney, 2002). In contrast to myosin V and myosin VI, which form dimers in solution and are processive, Myo1b is monomeric and non-processive (Stafford et al., 2005). In yeast, class-I myosins control endocytosis by regulating actin nucleation, whereas in *Dictyostelium discoidum* one member of this class is involved in membrane recycling, most probably by regulating the morphology of these compartments (Geli et al., 2000; Neuhaus and Soldati, 2000). Here, we present evidence for the role of Myo1b in the morphology of endosomes and in the trafficking of molecules in early sorting MVEs.

Myo1b and the morphology of early sorting MVEs

It is generally accepted that the cellular distribution of the endocytic compartments depends upon the balance between anterograde and retrograde microtubules-motors that bind to these compartments. However, we have previously reported that Myo1b contributes to the distribution of lysosomes and transferrin receptor labelled endosomes (Cordonnier et al., 2001; Raposo et al., 1999). Furthermore, we have also reported that Myo1b and actin filaments cooperate with microtubules for the movement of lysosomes (Cordonnier et al., 2001). Consistent with these observations we show here that Myo1b and actin filaments control the distribution of EEA1 labelled endosomes. Myo1b and the actin networks might act as part of the regulatory machinery that transiently retains the endocytic compartments on actin filaments during their travelling on microtubules.

EEA1 is associated with early endosomes and early sorting MVEs with a bilayered clathrin coat. Early sorting MVEs are important sorting stations for the proteins that are delivered to lysosomes or involved in the biogenesis of lysosomes related organelles such as melanosomes (Raposo and Marks, 2002; Raposo et al., 2001; Sachse et al., 2002). We report here that, overexpression of EGFP-Myo1b or treatment with drugs that perturbe the dynamics of the actin cytoskeleton highlighted the presence of numerous small membrane extensions at the surface of these endosomes. We therefore suggest that MYO1B and actin contribute to the morphology of these endocytic compartments. Several lines of evidence suggest that MYO1B binds to the membrane of the endosomes. Using electron microscopy, we have previously reported that Myo1b was associated with endosomes and lysosomes from an hepatoma cell line and report here that EGFP-Myo1b is found on EEA1 labelled early sorting MVEs. Myo1b was also detected in fractions enriched with endosomes isolated from the hepatoma cell line (Raposo et al., 1999) and from MNT-1 cells (this study). Furthermore, we have previously shown that Myo1b was released from membrane fractions in the presence of the tail-domain of this molecular motor, suggesting that the interaction of Myo1b with membranes is mediated by this domain. In parallel, recent observations suggest that in solution, Myo1b regulates the organisation of actin filaments (Stafford et al., 2005). At low concentrations of Myo1b actin filaments are straighter and at high concentrations they form bundles. Modification of the cellular organisation of the actin network was never observed in the presence of EGFP-Myo1b at light microscopic level. However, we cannot exclude that MYO1B regulates the organisation of actin filaments at the surface of the early sorting MVE. In interacting with the membrane of endosomes on one hand and actin filaments on the other, MYO1B might transiently retain endosomes on actin filaments and exert tension on the endosomal membrane to form the small membrane extensions observed at the EM level.

Myo1b and the traffic of proteins that pass through early sorting MVEs

By controlling the morphology of the sorting MVE, MYO1B might participate in the trafficking of those proteins that exist in these endocytic compartments. The peculiar processing of Pmel17 allowed us to study the impact of the expression of EGFP-Myo1b in the traffic of proteins that are passing through these endocytic compartments. We found that, the expression of EGFP-Myo1b impaired the cellular distribution of Pmel17, delayed its proteolytic cleavage and, thereby, the maturation of melanosomes (Berson et al., 2001; Berson et al., 2003; Sachse et al., 2002). Furthermore, MYO1B associated to endosomes that co-immunoprecipitated with the precursor P2 of Pmel17. Consistent with the previous observations, which suggest that the interaction of Myo1b with membranes is mediated by its tail, this domain co-imunoprecipitates also with Pmel17. MYO1B might bind directly to the cytoplasmic domain of Pmel17 through its tail-domain or, these two proteins might belong to the same protein complex at the surface of the early sorting MVE. The interaction with the precursor P2 of Pmel17 might allow MYO1B to transiently retain P2 on the external membrane of the early sorting MVE and thereby prevent it from proteolytic cleavage. The interaction with Pmel17 on one hand and with actin filaments on the other might allow MYO1B to act as a dynamic scaffold that clusters proteins to be transported towards lysosomes through internal vesicles.

Altogether, the experimental evidence reported here strongly suggests that, MYO1B and actin filaments at the surface of MVEs act as a mechanical device that contribute to the morphology of these endocytic compartments and to the sorting of proteins that are transported to the internal vesicles of MVEs.

The machinery involved in sorting of protein cargos towards internal vesicles of MVEs has been recently unravelled in the case of ubiquitinated proteins. Cargo proteins are recognized at the cytosolic side of endosomes by a protein complex, called ESCRT-0, which contains HRS (mammalian hepatocyte receptor tyrosine kinase substrate) STAM (signal transduction adaptor molecule) and Eps15 (Raiborg et al., 2003). In this model HRS recruits Tsg101, a component of the ESCRT-I complex that in turn recruits the protein complexes ESCRT-II

and ESCRT-III. These protein-complexes act together to sequester ubiquitinated cargo proteins into the inward-budding vesicles of the MVEs (Bache et al., 2003; Lu et al., 2003). Some non-ubiquitinated proteins, however, are also delivered to the internal vesicles of MVEs (Reggiori and Pelham, 2001). A recent report indicates that HRS, but not Tsg101, is required for the transport of one of these proteins towards lysosomes (Hislop et al., 2004). Pmel17 might belong to this second class of proteins because we have not been able to detect an ubiquitin motif on this protein (data not shown). The acto-Myo1b-based mechanism might represent a part of the alternative machinery to sort non-ubiquitinated proteins in specific membrane domains at the cytosolic side of endosomes. Alternatively – or additionally – the retention of the proteins to be sorted in specific membrane domains at the surface of endosomes by an acto-Myo1b-based mechanism, might constitute an additional step in the trafficking events occurring in sorting MVEs.

We thank Catherine Martin for performing electronic microscopic analysis of actin in the vicinity of early MVE, Sophie Neveu for kindly preparing the magnetic nanoparticles and Marie-Thérèse Prospéri for preparing anti-MYO1b antibodies. We are grateful to Matthew Morgan for critical reading of the manuscript, and Michael Marks for fruitful discussions. This work was supported by a grant to E.C. from the association pour la recherche sur le Cancer (ARC n°4623). F.Y. and L.C.S. were successively the recipient of a grant from the Institut Curie.

References

Bache, K. G., Brech, A., Mehlum, A. and Stenmark, H. (2003). Hrs regulates multvesicular body formation via ESCRT recruitment to endosomes. *J. Cell Biol.* **162**, 435-442.

Berson, J. F., Harper, D., Tenza, D., Raposo, G. and Marks, M. S. (2001). Pmel17 initiates premelanosomal striation formation within multivesicular bodies. *Mol. Biol. Cell* **12**, 3451-3464.

Berson, J. F., Theos, A. C., Harper, D., Tenza, D., Raposo, G. and Marks, M. S. (2003). Proprotein convertase cleavage liberates a fibrillogenic fragment of a resident glycoprotein to initiate melanosome biogenesis. *J. Cell Biol.* **161**, 1-15.

Buss, F., Arden, S. D., Lindsay, M., Luzio, J. P. and Kendrick-Jones, J. (2001). Myosin VI isoform localised to clathrin coated vesicles with a role in clathrin mediated endocytosis. *EMBO J.* **20**, 3676-3684.

Cordonnier, M.-N., Dauzonne, D., Louvard, D. and Coudrier, E. (2001). Actin filaments and Myosin I alpha cooperate with microtubules for the movement of lysosomes. *Mol. Biol. Cell* **12**, 4013-4029.

Durrbach, A., Raposo, G., Tenza, D., Louvard, D. and Coudrier, E. (2000). Truncated brush border myosin I affects membrane traffic in polarized epithelial cells. *Traffic* **1**, 411.

Geli, M. I., Lombardi, R., Schmelzl, B. and Riezman, H. (2000). An intact SH3 domain is required for myosin I-induced actin polymerization. *EMBO J.* **19**, 4281-4291.

Hales, C. M., Vaerman, J.-P. and Goldering, J. R. (2002). Rab 11 family interacting protein 2 associates with myosin Vb and regulates plasma membrane recycling. *J. Biol. Chem.* **277**, 50415-50421.

Hasson, T. (2003). Myosin VI: Two distinct roles in endocytosis. *J. Cell Sci.* **116**, 3453-3461.

Hislop, J. N., Marley, A. and von Zastrow, M. (2004). Role of mammalian vacuolar protein-sorting proteins in endocytic trafficking of a non ubiquitinated G protein-coupled receptor to lysosomes. *J. Biol. Chem.* **279**, 22522-22531.

Hopkins, C. R., Gibson, A., Shipman, M., Strickland, D. K. and Trowbridge, I. S. (1994). In migrating fibroblasts, recycling receptors are concentrated in narrow tubules in the pericentriolar area, and then routed to the plasma membrane of the leading lamella. *J. Cell Biol.* **125**, 1265-1274.

Koster, G., VanDuijn, M., Hofs, B. and Dogterom, M. (2003). Membrane tube formation from giant vesicles by dynamic association of motor protein. *Proc. Natl. Acad. Sci. USA* **100**, 15583-15588.

Lu, Q., Hope, W. H., Brasch, M., Reinhard, C. and Cohen, S. N. (2003). TSG101 interaction with HRS mediates endosomal trafficking and receptor down regulation. *Proc. Natl. Acad. Sci. USA* **100**, 7626-7631.

Marks, M. S., Roche, P. A., van Donselaar, E., Woodruff, L., Peters, P. J. and Bonifacino, J. S. (1995). A lysosomal targeting signal in the cytoplasmic tail of the beta chain directs HLA-DM to MHC class II compartments. *J. Cell Biol.* **131**, 351-369.

Neuhaus, E. M. and Soldati, T. (2000). A myosin I is involved in membrane recycling from early endosomes. *J. Cell Biol.* **150**, 1013-1026.

Raiborg, C., Rusten, T. E. and Stenmark, H. (2003). Protein sorting into multivesicular endosomes. *Curr. Opin. Cell Biol.* **15**, 446-455.

Raposo, G. and Marks, M. S. (2002). The dark side of lysosome-related organelles: specialization of the endocytic pathway for melanosome biogenesis. *Traffic* **4**, 237-248.

Raposo, G., Tenza, D., Mecheri, S., Peronet, R., Bonnerot, C. and Desaymard, C. (1997). Accumulation of major histocompatibility complex class II molecules in mast cell secretory granules and their release upon degranulation. *Mol. Biol. Cell* **12**, 2631-2645.

Raposo, G., Cordonnier, M. N., Tenza, D., Menichi, B., Durrbach, D., Louvard, D. and Coudrier, E. (1999). Association of myosin I with endosomes and lysosomes in mammalian cells. *Mol. Biol. Cell* **10**, 1477-1494.

Raposo, G., Tenza, D., Murphy, D. M., Berson, J. F. and Marks, M. S. (2001). Distinct protein sorting and localization to premelanosomes, melanosomes, and lysosomes in pigmented melanocytic cells. *J. Cell Biol.* **152**, 809-824.

Reggiori, F. and Pelham, H. R. B. (2001). Sorting of proteins into multivesicular bodies: ubiquitin-dependent and -independent targeting. *EMBO J.* **20**, 5176-5186.

Rodriguez, O. and Cheney, R. (2002). Human myosin-Vc is a novel class V myosin expressed in epithelial cells. *J. Cell Sci.* **115**, 991-1004.

Roux, A., Cappello, G., Cartaud, J., Prost, J., Goud, B. and Bassereau, P. (2002). A minimal system allowing tubulation with molecular motors pulling on giant liposomes. *Proc. Natl. Acad. Sci. USA* **99**, 5394-5399.

Ruppert, C., Kroschewski, R. and Bähler, M. (1993). Identification, characterization and cloning of myr **1**, a mammalian Myosin-1. *J. Cell Biol.* **120**, 1393-1403.

Sachse, M., Urbé, S., Oorshot, V., Strous, G. and Klumperman, J. (2002). Bilayered clathrin coats on endosomal vacuoles are involved in protein sorting toward lysosomes. *Mol. Biol. Cell* **13**, 1313-1328.

Stafford, W. F., Walker, M. L., Trinick, J. A. and Coluccio, L. M. (2005). Mammalian class I myosin, Myo1b, is monomeric and cross-links actin filaments as determined by hydrodynamic studies and electron microscopy. *Biophys. J.* **88**, 384-391.

Stoorvogel, W., Geuze, H. and Strous, G. (1987). Sorting of endocytosed transferrin and asialoglycoprotein occurs immediately after internalization in HepG2 cells. *J. Cell Biol.* **104**, 1261-1268.

Stoorvogel, W., Oorschot, V. and Geuze, H. J. (1996). A novel class of clathrin-coated vesicles budding from endosomes. *J. Cell Biol.* **132**, 21-33.

Tang, N. and Ostap, E. M. (2001). Motor domain-dependant localisation of myo1b (myr-1). *Curr. Biol.* **11**, 1131-1135.

Wilhelm, C., Gazeau, F., Roger, J., Pons, J., Billotey, C. and Bacri, J. (2002). Interaction of anionic superparamagnetic nanoparticles with cells: kinetic analysis of membrane adsorption and subsequent internalization. *Langmuir* **18**, 8148-8155.